Nonlinear-transmission dynamics and nonlinear susceptibilities of semiconducting microcrystals (quantum dots)

Yu. V. Vandyshev, V. S. Dneprovskiĭ, and V. I. Klimov

Moscow State University

(Submitted 3 July 1991)
Zh. Eksp. Teor. Fiz. **101**, 270–283 (January 1992)

Bleaching peaks associated with transitions between quantum-well levels have been detected in the nonlinear transmission spectra of semiconducting CdSe microcrystals of various radii. The process by which the transmission is restored has been studied. It is explained in terms of a filling of quantum-well levels by carriers excited by picosecond laser pulses. A gain regime has been detected for the first time in semiconductor quantum dots. This gain is manifested in both the nonlinear transmission spectra and the luminescence spectra. The dispersion of the real and imaginary parts of the cubic susceptibility is determined. The nonlinear-optics constants are determined as functions of the size of the microcrystals and the carrier lifetime.

INTRODUCTION

Semiconducting microcrystals are quasi-zero-dimensional structures (quantum dots), whose energy spectrum differs substantially from that of bulk semiconductors.[1] In microcrystals whose radius is small (in comparison with the exciton radius), the quantum size effect gives rise to discrete energy levels in the conduction and valence bands. Transitions between these levels should be manifested as separate absorption peaks. It is difficult to observe this discrete spectral structure, however, because of the pronounced inhomogeneous broadening of the quantum-well levels caused by the scatter in the size and shape of the microcrystals. In the case of CdSe and CdS_xSe_{1-x}, for example, it is only in microcrystals of extremely small diameter (4–5 nm at the largest) that one observes in the linear absorption spectra the weak oscillations[2,3] associated with transitions between pairs of low-lying levels in the conduction band and the three valence subbands ($1s$–$1s$ transitions).

The resonant dynamic nonlinearities detected in microcrystals are associated with a short-wave shift of the absorption edge of the semiconductor,[4] which apparently results from a filling of low-lying quantum-well levels by photoexcited carriers. In semiconductor quantum-dot structures (heterostructures with quantum wells and superlattices), the quantum size effect gives rise to a substantial increase in the characteristic nonlinear-optics constants.[5] Calculations show that a corresponding effect should occur for microcrystals, in the case of an independent quantization of the electron and hole energies (in microcrystals of small radius)[6] and also in the case of an energy quantization of the translational motion of an exciton (in comparatively large microcrystals).[7] However, the values which have been detected for the cubic nonlinear susceptibility $\chi^{(3)}$ of these microcrystals do not exceed[3,8] 10^{-7}–10^{-8} esu. These values are well below the values of $\chi^{(3)}$ of bulk semiconductors. On the one hand, this circumstance can be attributed to the low concentration by volume of the semiconductor in the test samples (up to 1%). On the other, it can be attributed to the short carrier lifetimes, which are lowered to hundreds or even tens of picoseconds during intense pumping.[9,10] We might add that in place of the expected increase in $\chi^{(3)}$ with decreasing size of the microcrystals one usually observes the opposite effect.[2] This result may be a consequence of a pronounced reduction of the carrier lifetime in small-radius microcrystals as the result of an increase in the efficiency of radiationless recombination.

In the present paper we examine the dynamics of the nonlinear-transmission spectra of a glass doped with CdSe microcrystals. In these crystals, a quantum-well level structure is exhibited as the result of a selective excitation of the microcrystals. This structure is not seen in the linear transmission spectra. The spectra of induced changes in the absorption coefficient which have been detected have been used to determine the dispersion of the induced refractive index and the spectra of the real and imaginary parts of the cubic susceptibility. The effect of the microcrystal size (for the case in which the radius of the microcrystals does not exceed the first Bohr radius of the exciton) and that of the carrier lifetime on the typical values of the nonlinear-optics constants are studied.

EXPERIMENTAL PROCEDURE

We studied samples of a glass doped with CdSe (at $T = 80$ K) with microcrystal radii ranging up to 10 nm. The crystals were excited by ultrashort pulses at the second harmonic of a mode-locked neodymium ($YAG:Nd^{3+}$) laser, with a photon energy $\hbar\omega_0 = 2.33$ eV. The length of an individual pump pulse was 20–25 ps, and its energy W was up to 0.5 mJ. The exciting light was directed along the normal to the surface of the sample and was focused into a spot 0.5–2 mm in diameter. The central part of the excitation region was probed by an oppositely directed collinear beam of "white" light, produced by sending ultrashort pulses at the fundamental frequency of a laser with a wavelength of 1.06 μm into a cell filled with heavy water. Two delay lines (in the excitation and probing channels) made it possible to delay the probing pulse with respect to the exciting pulse by a time ranging up to 3 ns. The probing light was detected (in front of and behind the sample) by an OVA-284 multichannel analyzer, with a signal buildup of 50–100 pulses and with energy selection of the ultrashort excitation pulses within an error $\pm$ 10%. In these experiments we measured the differential transmission spectra

$$DT(\lambda) = \frac{T(\lambda) - T_0(\lambda)}{T_0(\lambda)} \qquad (1)$$

[$T(\lambda)$ and $T_0(\lambda)$ are the transmission spectra of the excited and unexcited sample, respectively]. We were thus able to

 0038-5646/92/010144-07$05.00

eliminate the effect of the spectral characteristics of the photodetectors on the final results and to reduce the role played by an instability of the spectral composition of the probing light. [Transmission spectra normalized to the reference spectra of the probing light were used in (1)].

EXPERIMENTAL RESULTS AND DISCUSSION

1. Dynamics of the differential transmission spectra

Figure 1, a and b, shows DT(λ) spectra for two samples, 1 and 2, with microcrystals of different radii $R_1 > R_2$. (The corresponding linear-transmission spectra are shown by the dashed lines in Fig. 1.) The exciting pulse causes a pronounced bleaching near the absorption edge of the samples. With an increase in the delay time Δt, the spectral region in which the bleaching is observed becomes narrower, and the short-wave edge of the DT(λ) spectrum moves to a lower energy. The long-wave edge remains at essentially the same position.

A distinctive feature of the DT(λ) spectra is a characteristic discrete structure, which is not seen in the linear absorption spectra. The spectrum of sample 1 has some well-resolved bleaching peaks at $\lambda_1 = 649$ nm, $\lambda_2 = 616$ nm, and $\lambda_3 = 563$ nm; sample 2 has a peak at $\lambda_1' = 585$ nm. (Near the λ_1 and λ_2 bands, we observe not a simple bleaching but a fairly significant gain, which is close in magnitude to the absorption coefficient of the unexcited sample.) The relaxation times of the induced bleaching were very different in the test samples. In sample 2, the transmission recovery time was about 100 ps, while the transmission of sample 1 had not recovered completely even after the maximum delay of 3 ns.

Pronounced differences were found in the dynamics of the transmission relaxation at the different bleaching bands. This situation is particularly clear in the case of sample 1. Band λ_3 disappears from the DT(λ) spectrum nearly completely during the first 70 ps after the application of the ultrashort excitation pulse, while band λ_2 increases in amplitude over this time interval and then decays over about 2 ns. The longest-lived peak, λ_1, does not relax completely even at the maximum delay values, $\Delta t = 3$ ns.

The presence of well-defined bleaching peaks in the DT(λ) spectra and the differences in their decay dynamics can be explained by a model for the filling of the quantum-well levels which form in the valence and conduction bands during the independent quantization of the electron energy and the hole energy. The positions of the absorption peaks associated with transitions between these levels are given by[1]

$$E_{i,l,n} = E_g^i + \frac{\hbar^2 \varphi_{l,n}^2}{2m_r R^2},$$

where E_g^i is the width of the band gap associated with subband i of the valence band ($i = A,B,C$), $m_r = m_e m_h/(m_e + m_h)$ (m_e and m_h are the effective carrier masses), and $\varphi_{l,n}$ is the nth root of the Bessel function $J_{l+1/2}$. Bleaching peaks λ_1 and λ_2 for sample 1 essentially coincide with the energies $E_{0,1}$ and $E_{1,1}$ of the first two transitions (1s–1s and 1p–1p) for R at about 6 nm. The λ_3 peak lies in the region of transitions with energies $E_{2,1}$, $E_{0,2}$, and $E_{3,1}$. The position of the λ_1' peak for sample 2 corresponds to the energy $E_{0,1}$ of the 1s–1s transition with R at about 3.5 nm.

Evidence in favor of a high efficiency for the filling of the levels comes from the fact that a significant gain is observed in bands λ_1 and λ_2 (in sample 1). At small values of Δt, this gain reaches values approaching the maximum possible value. The absorption coefficient in the region of the transition from the (l,n) level of valence subband i to the (l,n) level of the conduction band can be written as follows, according to our model for the filling of levels:

$$\alpha_{i,l,n} = \alpha_{i,l,n}^0 (1 - n_{l,n}^e - n_{i,l,n}^h), \qquad (2)$$

where $\alpha_{i,l,n}^0$ is the absorption coefficient of the unexcited sample, which is proportional to the degree of degeneracy of the levels under consideration [$2(2l+1)$], and $n_{l,n}^e$ and $n_{i,l,n}^h$ are the occupation numbers of the levels in the conduction and valence bands, respectively. If the sum of occupation numbers ($n_{l,n}^e + n_{i,l,n}^h$) exceeds one, the system does not absorb. It instead amplifies the light. The maximum value of the gain g, which is reached under the condition

$$n_{l,n}^e = n_{i,l,n}^h = 1,$$

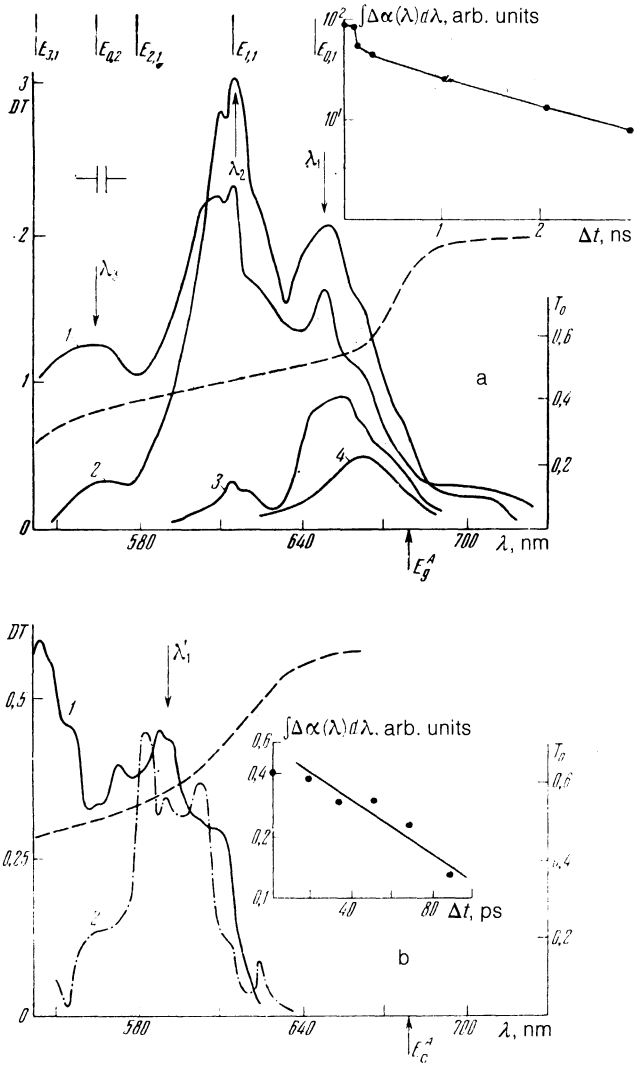

FIG. 1. Differential transmission spectra of CdSe microcrystals (at 80 K). a: Sample 1, $W = 0.12$ mJ. 1—$\Delta t = 0$; 2—66 ps; 3—1 ns; 4—2 ns. b: Sample 2, $W = 0.25$ mJ. 1—$\Delta t = 0$; 2—33 ps. The solid line shows the transmission spectra of unexcited samples. The insets illustrate the temporal changes in the integral $\int \Delta\alpha(\lambda)d\lambda$, which is proportional to the total number of photoexcited electron-hole pairs in a microcrystal.

turns out to be equal to the absorption coefficient of the unexcited sample: $g_{\max} = \alpha^0_{i,l,n}$. In this case the differential transmission is at a maximum and is given by

$$DT_{max} = \frac{r^4}{T_0^2} - 1$$

(r is the reflection coefficient at one face of the sample). Near the λ_2 peak we have $T_0 = 0.46$ and thus $DT_{max} = 3$ (with $r = 0.96$). This value is essentially the same as the measured value of $DT(\lambda_2)$ at $\Delta t = 66$ ps (Fig. 1a).

Gain effects are also seen clearly in the luminescence spectra.[11] At $W > 20$ μJ, a comparatively narrow peak of amplified luminescence appears at the crest of a broad spontaneous-emission band. A scattering of the amplified light is clearly visible at the faces of the sample under these conditions.[1)]

To determine the relaxation characteristics of the electron-hole system in a microcrystal, we studied the time evolution of the induced difference in absorption coefficients,

$$\Delta\alpha(\lambda) = \alpha(\lambda) - \alpha_0(\lambda)$$

in the various bleaching bands. In our filling model, the value of $\Delta\alpha$ near the (i,l,n)–(l,n) transition is proportional to the number of carriers in the corresponding states of the valence and conduction bands [see (2)]. The total number of photoexcited carriers is proportional here to the integral $\int \Delta\alpha(\lambda) d\lambda$. The time evolution of this integral is shown in the insets in Fig. 1, a and b (see also the data of Ref. 11).

The fast relaxation of the λ_3 peak {with a time scale $\tau = -\Delta\alpha[d(\Delta\alpha)/dt]^{-1}$ of about 60 ps} observed in the initial stage ($\Delta t < 70$ ps) for sample 1, on the one hand, and the negligible increase in the amplitude of the λ_2 and λ_3 bands, on the other, can be attributed to a cooling of the carriers accompanying their transition from the higher-lying states to the two lower-lying states. The integral of $\Delta\alpha$ varies only negligibly (see the inset in Fig. 1a), implying a slight decrease in the total number of photoexcited electron-hole pairs. The subsequent behavior of the system ($\Delta t > 70$ ps) is apparently governed by a recombination of carriers (spectra 3 and 4 in Fig. 1a), in the course of which the λ_2 peak disappears (the time scale τ for this peak increases with increasing Δt from 300 to 700 ps), and the longest-lived band, λ_1, undergoes a partial relaxation. The value of $\Delta\alpha$ for this band falls off essentially exponentially with a time scale of about 2 ns. For the integral of $\Delta\alpha$, as for the λ_2 band, we see a transition from a very nonexponential decay to an essentially exponential decay. As the reasons for the nonexponential decay of the electron-hole system in the microcrystals we might cite nonlinear recombination mechanisms (e.g., an Auger process[9]) or induced-emission effects.

The relaxation times measured for sample 2 are considerably shorter. In particular, the decrease in the integral of $\Delta\alpha$ occurs with a time scale of only about 60 ps.

The lifetime τ of the electron-hole pairs in a microcrystal is determined by the joint effects of radiative and radiationless recombination. This lifetime can be written

$$\tau = \frac{\tau_r \tau_{nr}}{\tau_r + \tau_{nr}},$$

where τ_r and τ_{nr} are the time scales for radiative and nonradiative decay, respectively. With an independent quantization of the electron and hole energies, the oscillator strength for the allowed transition per microcrystal and thus the radiative-recombination time τ_r are independent of the size of the microcrystals.[7] Estimates show[9] that the time τ_r for CdSe is about 1–2 ns. The time scale τ of the exponential decay measured for sample 1 is 2 ns, close to the value of τ_r. This approximate agreement is evidence that radiative processes are highly efficient (this conclusion is supported by the presence of the intense stimulated emission found in the case of sample 1). For sample 2, the time τ is considerably shorter than τ_r. It can be concluded on this basis that there is a predominantly nonradiative recombination in this case (at $\tau \ll \tau_r$, the decay time is $\tau \approx \tau_{nr}$). The increase in the importance of nonradiative processes with decreasing radius of the microcrystals can apparently be attributed to an increase in the efficiency of recombination through surface states.[8]

2. Calculations of the nonlinear-transmission spectra of the microcrystals

According to our model for the filling of levels, the absorption spectrum of the excited sample can be determined by summing the contributions [see (2)] from all allowed transitions between quantum-well levels in the conduction band and in the three valence subbands of the semiconductor:

$$\alpha(\hbar\omega) = G \sum_{i,l,n} f_i (2l+1) \int_0^\infty (1 - n^e_{l,n} - n^h_{i,l,n}) g(\hbar\omega - E_{i,l,n}) P(R) dR. \quad (3)$$

Here $g(\hbar\omega - E_{i,l,n})$ is a spectral factor which accounts for the homogeneous broadening of the transition between a pair of separate quantum-well levels; $P(R)$ is the size distribution of the microcrystals, which describes inhomogeneous-broadening effects; f_i are oscillator strengths for transitions between the conduction band and the various valence subbands, averaged over polarization; and G is a constant. In the course of the calculations, this constant was chosen by fitting calculated absorption spectra of the unexcited sample, $\alpha_0(\hbar\omega)$, to the measured spectra.

For comparison with experimental results, we used (3) to calculate the absorption spectra of the excited and unexcited samples. We then calculated the differential transmission spectra under the assumption that inhomogeneous broadening is predominant. The latter assumption makes it possible to replace the spectral factor $g(\hbar\omega - E_{i,l,n})$ in (3) by a δ-function $\delta(\hbar\omega - E_{i,l,n})$. To describe the inhomogeneous broadening, we use the size distribution of the microcrystals which was found by Lifshitz and Slezov.[12] The occupation numbers were found under the assumption of a quasiequilibrium Fermi energy distribution with a certain electron temperature T_e and with N excited electron-hole pairs, the same in all the microcrystals. The electron and hole chemical potentials were calculated from

$$\sum_{l,n} 2(2l+1) n^e_{l,n} = N, \quad \sum_{i,l,n} 2(2l+1) n^h_{i,l,n} = N. \quad (4)$$

Figure 2 shows the results of numerical calculations of the spectra $DT(\lambda)$, i.e.,

$$DT(\lambda) = \exp[(\alpha_0(\lambda) - \alpha(\lambda))d] - 1,$$

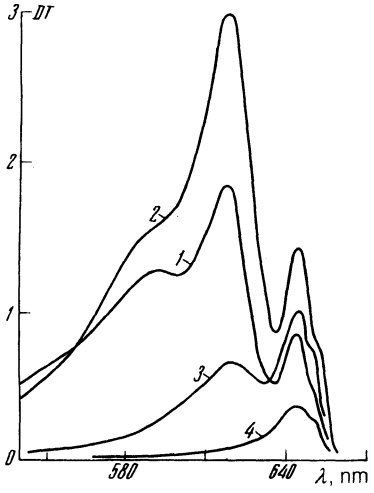

FIG. 2. Calculated differential transmission spectra of CdSe microcrystals (average radius $\bar{R} = 5$ nm). 1—$T_e = 500$ K; 2–4—80 K. 1, 2) $N = 12$; 3) 4; 4) 1.

(d is the thickness of the sample), for samples with an average microcrystal radius $R = 5$ nm (sample 1). The spectra calculated for N between 12 and 1 provide a good explanation of the shape and dynamics of the experimental $DT(\lambda)$ spectra. In the calculated spectra, as in the experimental spectra, we clearly see two bleaching (or gain) peaks, associated with transitions between pairs of low-lying $1s$ and $1p$ electron and hole levels. We also see a third peak, not as well defined, in the vicinity of the higher-lying levels which follow.

Spectra *1* and *2* in Fig. 2 were calculated for two different temperatures of the electron-hole system (500 and 80 K, respectively) at a fixed number of carriers in a microcrystal ($N = 12$). These spectra correspond to the cooling of the electron-hole system (see spectra 1 and 2 in Fig. 1a) observed in the initial stage ($\Delta t < 70$ ps). Spectra *2–4* were calculated at a fixed temperature $T_e = 80$ K and for various values of the total number of electron-hole pairs in a microcrystal. These spectra describe the dynamics of the $DT(\lambda)$ spectra in the course of the recombination (see the measured spectra *2–4* in Fig. 1a).

Despite the good agreement between the theoretical and experimental differential transmission spectra, the simplified calculation version described above leads to some fairly strong oscillations in the linear absorption spectra which are not observed experimentally. We would expect a closer agreement with the measured spectra from calculations incorporating both inhomogeneous and homogeneous broadening and also incorporating the differences in the number of electron-hole pairs excited in microcrystals of different radii. Under the experimental conditions, with the samples being pumped by narrow-band laser light (the linewidth was about 0.3 nm), not all of the microcrystals were excited. Only those microcrystals for which the center of the homogeneous-broadening line lay near the laser line were excited. Consequently, while the linear transmission spectra do not reveal the discrete structure associated with the size quantization, because of the joint effects of homogeneous and inhomogeneous broadening, the nonlinear transmission spectra reflect a substantially reduced role of inhomogeneous broadening because of the selective excitation of the microcrystals of a certain radius (a "hole was burned" in the size distribution of the microcrystals). It thus becomes possible to detect bleaching peaks whose width apparently corresponds to the homogeneous broadening of transitions between quantum-well levels.

3. Induced changes in the refractive index

Since the nonlinearities detected in the microcrystals stem primarily from large absorption changes near the absorption edge of the semiconductor, the corresponding refractive-index changes $\Delta n(\lambda)$ can be found from the measured spectra of the induced absorption coefficient $\Delta\alpha(\lambda)$ with the help of the Kramers-Kronig relations. In the case of small dispersion-related changes we can write

$$\Delta n(\lambda) = \frac{1}{2\pi^2} \int_0^\infty \frac{\Delta\alpha(x) - \Delta\alpha(\lambda)}{1-(x/\lambda)^2}\, dx.$$

The results calculated for the $\Delta n(\lambda)$ spectra corresponding to different delay times Δt are shown in Fig. 3a (for sample 1) and Fig. 3b [sample 2; the spectrum corresponding to $\Delta t = 0$ is not shown in Fig. 3b, since in this case a large part of the $\Delta\alpha(\lambda)$ spectrum falls near the lasing line]. The amplitude values of Δn are $\pm (3\text{–}4)\cdot 10^{-5}$ for sample 1 and $\pm 10^{-5}$ for sample 2. With increasing Δt, the $\Delta n(\lambda)$ spectra acquire the shape characteristic of a saturated two-level system.

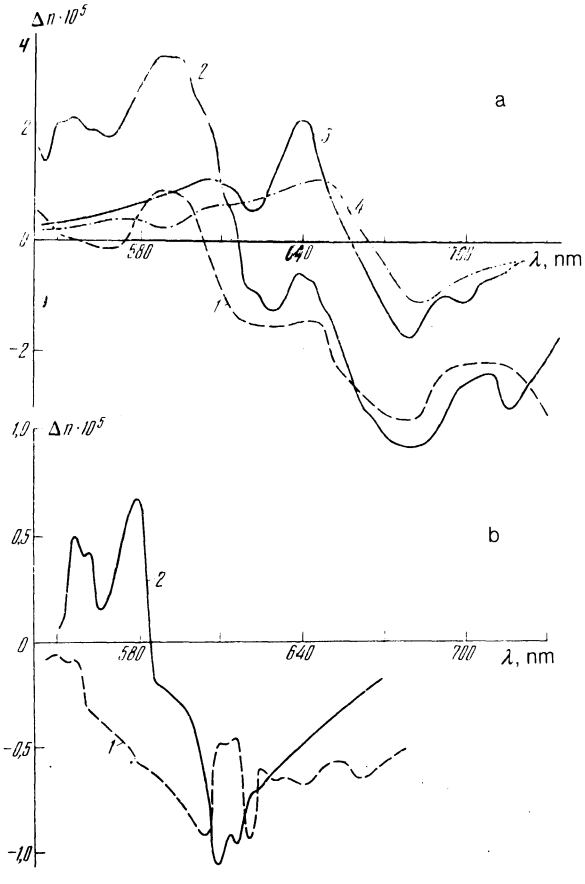

FIG. 3. Spectra of the induced changes in the refractive index, $\Delta n(\lambda)$. a: Sample 1. 1—$\Delta t = 0$; 2—66 ps; 3—1 ns; 4—2 ns. b: Sample 2. 1—$\Delta t = 17$; 2—33 ps.

4. Cubic-susceptibility spectra

The most informative characteristics of optically nonlinear media are their nonlinear susceptibilities. Glasses doped with microcrystals are isotropic media, so the only nonvanishing nonlinear susceptibilities are of odd order in this case: $\chi^{(3)}$, $\chi^{(5)}$, etc. In the devices which are used in practice, the nonlinear-optics elements work under self-action conditions. Responsible for processes of this sort are the so-called Kerr susceptibility $\chi^{(3)}(\omega;\omega,-\omega,\omega)$ [below we will write simply $\chi^{(3)}(\omega)$] and other higher-order susceptibilities with a similar set of frequencies.

The most common method for determining nonlinear characteristics of semiconductor-doped glasses is degenerate four-wave mixing.[13,14] That method, however, is capable of revealing only the absolute value of the susceptibility, $\chi^{(3)}$; auxiliary measurements are required to determine its phase.[15] Other disadvantages of that method are the difficulties in calibrating the signal so that absolute as well as relative measurements can be carried out. Another shortcoming is that measurements can be carried out only at certain fixed wavelengths.

The spectra $\mathrm{DT}(\lambda)$, $\Delta\alpha(\lambda)$, and $\Delta n(\lambda)$ obtained in the present study can be used to directly determine the spectra of the real and imaginary parts of the nonlinear susceptibility $\chi^{(3)}$. The changes in the susceptibility χ caused by a monochromatic field of frequency ω,

$$E = E_\omega e^{-i\omega t} + \text{c.c.}$$

can be written in the form

$$\Delta\chi(\omega) = \chi^{(3)}(\omega)|E_\omega|^2 + \chi^{(5)}(\omega)|E_\omega|^2 + \ldots$$

The real and imaginary parts of $\Delta\chi$ determine the induced changes in the absorption coefficient and the refractive index:

$$\Delta\alpha = \frac{4\pi\omega}{cn_0}\,\mathrm{Im}\,\Delta\chi, \qquad \Delta n = \frac{2\pi}{n_0}\,\mathrm{Re}\,\Delta\chi. \tag{5}$$

where n_0 is the linear refractive index. In the case of a relatively weak field, in which we can ignore processes of fifth and higher orders, the changes in χ are determined by the cubic susceptibility, and expressions (5) can be used to determine $\mathrm{Re}\,\chi^{(3)}$ and $\mathrm{Im}\,\chi^{(3)}$:

$$\mathrm{Re}\,\chi^{(3)}(\omega) = \frac{cn_0^2\,\Delta n(\omega)}{4\pi^2 I_\omega}, \qquad \mathrm{Im}\,\chi^{(3)}(\omega) = \frac{c^2 n_0^2\,\Delta\alpha(\omega)}{8\pi^2\omega I_\omega}, \tag{6}$$

where

$$I_\omega = \frac{cn_0|E_\omega|^2}{2\pi}$$

is the intensity of the monochromatic wave. When the measured Δn and $\Delta\alpha$ spectra are used in (6), it becomes necessary also to determine the corresponding spectrum I_ω. The latter is of course not the same as the spectrum of the laser light used in the experiments. It must instead be calculated by an approach which leads to the changes Δn and $\Delta\alpha$ observed experimentally under the conditions of the steady-state self-effect. Nonlinear changes in α and n are caused by the excitation of a certain number of electron-hole pairs N in a microcrystal [we wish to stress that we are talking about resonant dynamic (!) nonlinearities], so the I_ω spectrum can be found from the kinetic equation

$$\frac{dN}{dt} = \frac{I_\omega(1-T(\omega)-r)}{\hbar\omega\,dN_m}\frac{N}{\tau_e}. \tag{7}$$

In the steady state we have

$$I_\omega = \frac{N\hbar\omega\,dN_m}{\tau_e(1-T(\omega)-r)},$$

where N_m is the concentration of microcrystals ($N_m = \xi/V_m$, where ξ is the concentration by volume of the semiconductor, and V_m is the volume of a microcrystal), τ_e is the lifetime of the nonequilibrium electron-hole pairs when all possible recombination mechanisms are taken into account, and

$$T(\omega) = T_0(\omega)(1+D\mathrm{T}(\omega))$$

is the transmission spectrum of the excited sample. All the spectra ($\Delta\alpha(\omega)$, $\Delta n(\omega)$, and I_ω, which appear in expressions (6) for $\mathrm{Re}\,\chi^{(3)}$ and $\mathrm{Im}\,\chi^{(3)}$ can thus be expressed in terms of the experimental $T_0(\lambda)$ and $\mathrm{DT}(\lambda)$ spectra.

There are some points which need to be kept in mind when the procedure outlined above is used to calculate nonlinear-susceptibility spectra. As we mentioned earlier, the initial expressions, (6), are valid only for small changes in α and n, i.e., under conditions such that the cubic nonlinearity is predominant. These expressions therefore cannot be used at small delay times Δt, which correspond to large changes in the transmission and even to a gain regime, which is unattainable in principle under self-effect conditions. In practice, the $\mathrm{Re}\,\chi^{(3)}$ and $\mathrm{Im}\,\chi^{(3)}$ spectra were calculated through the use of the $\mathrm{DT}(\lambda)$ spectra, which show no evidence of gain. The changes in transmission were localized in the region of the transition between the first quantum-well levels.

A determination of absolute values of the nonlinear susceptibilities by the method outlined above presupposes the use of such parameters of the excited electron-hole system as the total number N, of electron-hole pairs, and the carrier lifetime τ_e. The time τ_e is apparently close to the measured relaxation time of the integral $\int\Delta\alpha(\lambda)d\lambda$, which is proportional to the total number of photoexcited carriers. The value of N can be found on the basis of the following considerations. At large values of Δt, at which the nonlinear changes in transmission are caused by a filling of the first quantum-well levels in the valence and conduction bands (these are the spectra which were used to calculate the nonlinear susceptibilities), the total number of electron-hole pairs in a microcrystal, N ($N = 2n^e = 2n^h$, where n^e and n^h are the occupation numbers of the low-lying levels), can be determined from the change in the absorption in the peak λ_1 (or λ_1') found experimentally: $\Delta\alpha = \alpha_0(n^e + n^h) = \alpha_0 N$. Hence, $N = \Delta\alpha/\alpha_0$.

Figure 4, a and b, shows $\mathrm{Re}\,\chi^{(3)}$ and $\mathrm{Im}\,\chi^{(3)}$ spectra found for samples 1 and 2 by the method outlined above. In an earlier study, Roussignol *et al.*[15] pointed out that there was no resonance structure in the nonlinear-susceptibility spectra. In contrast, our own spectra are clearly resonant. The reason lies in the presence of a clearly defined discrete structure in the $\mathrm{DT}(\lambda)$ spectra. As in the case of the ordinary saturating two-level system,[16] the values of $\mathrm{Re}\,\chi^{(3)}$ at frequencies below the resonant frequency are negative, while those above the resonant frequency are positive. The $\mathrm{Im}\,\chi^{(3)}$ spectrum lies entirely in the region of negative values. This

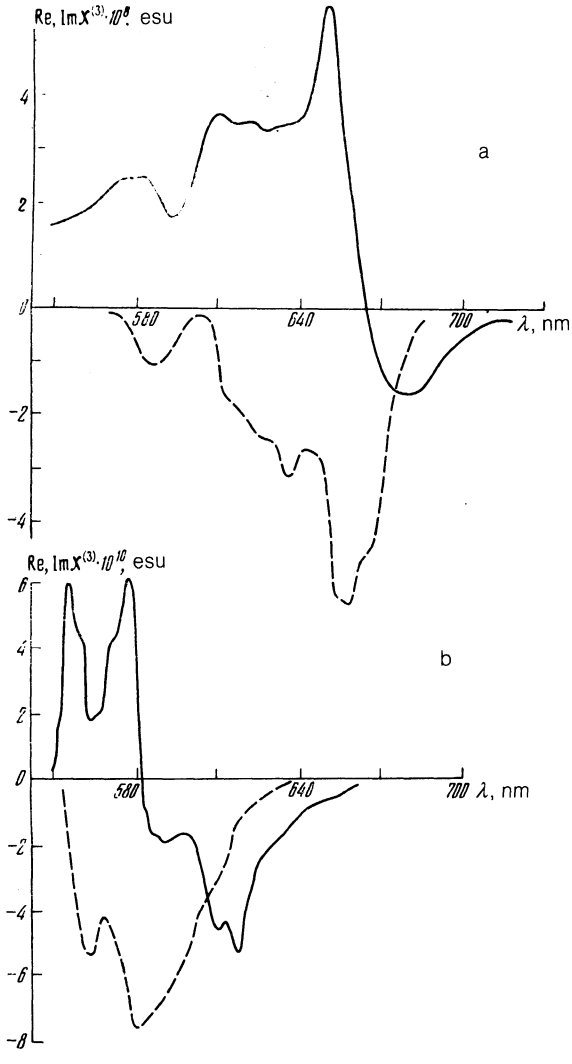

FIG. 4. Spectra of the real part (solid line) and imaginary part (dashed line) of the cubic susceptibility $\chi^{(3)}(\lambda)$ for samples 1 (a) and 2 (b).

situation corresponds to a predominant role of the bleaching effect. The amplitude values of the real and imaginary parts of the cubic susceptibility are comparable in magnitude, about $6 \cdot 10^{-8}$ esu in the case of sample 1 and $7 \cdot 10^{-10}$ esu for sample 2.

We can work from the spectra of the nonlinear susceptibilities to determine other nonlinear-optics parameters of these materials, e.g., the nonlinear refractive index n_2 and the saturation intensity I_s [determined from the condition $\Delta\alpha(I = I_s) = \alpha_0/2$]. For sample 1, the amplitude values of n_2 are $3.3 \cdot 10^{-7}$ cm^2/kW ($\lambda = 649$ nm) and $-0.9 \cdot 10^{-7}$ cm^2/kW ($\lambda = 680$ nm). The minimum value of I_s is about 0.1 MW/cm^2 ($\lambda = 658$ nm).

The values found for the nonlinear susceptibilities are well below the values characteristic of bulk CdSe crystals. In a study of the saturation of exciton absorption in CdSe (at 80 K), Zimin *et al.*[17] found $I_s = 30$ kW/cm^2. This figure corresponds to an Im $\chi^{(3)}$ value of about 10^{-3} esu, several orders of magnitude higher than $\chi^{(3)}$ for sample 1. However, the nonlinear parameters determined in the present study were calculated per unit volume of the doped glass, only a small fraction of which consists of the nonlinear material (ξ is about 0.1%). The nonlinear susceptibilities per unit volume of the semiconductor of these samples are larger by a factor of $1/\xi$. In the case of sample 1, they reach values of about 10^{-4} esu, close to the corresponding values for a bulk semiconductor. The pronounced decrease in the nonlinear susceptibilities in the case of sample 2, with smaller microcrystals (this decrease stands in contrast with the increase in the nonlinearities which was predicted in Ref. 6), is apparently due to a sharp reduction of the carrier lifetime (from 2 ns for sample 1 to 60 ps for sample 2).

Let us use our level-filling model to estimate the nonlinear susceptibilities of the semiconductor microcrystals. In the case of an independent quantization of the electron and hole energies (in small-radius microcrystals), transitions between states of the valence band and states of the conduction band with identical sets of quantum numbers (l,n) are dipole-allowed. The dipole matrix elements of such transitions are the same. They are also equal to the matrix element d_i (i is the index of the valence subband) of an interband transition in a bulk semiconductor.[7] The susceptibility of an excited sample in this case (with inhomogeneous broadening ignored) can be written

$$\chi(\hbar\omega) = N_m \sum_{i,l,n} |d_i|^2 \frac{2(2l+1)\,(n^e_{l,n} + n^h_{i,l,n} - 1)}{(\hbar\omega - E_{i,l,n}) + i\hbar\Gamma_{i,l,n}}, \qquad (8)$$

where $\Gamma_{i,l,n}$ is the homogeneous linewidth for a transition between two separate quantum-well levels in the valence band and the conduction band. Under the assumption of a quasiequilibrium Fermi distribution, the occupation numbers $n^e_{l,n}$ and $n^h_{i,l,n}$ are determined by the electron temperature of the electron-hole system and by the total number of photoexcited carriers, N. At moderate excitation levels, carrier heating can be ignored, and T_e can be set equal to the lattice temperature. The value of N can be found from the kinetic equation discussed above, (7). In the case of steady-state excitation, that equation gives us

$$N = \frac{\tau_e \alpha(\omega) I_\omega}{\hbar\omega N_m} = \frac{2\tau_e |\operatorname{Im}\chi(\omega)|}{\hbar N_m} |E_\omega|^2. \qquad (9)$$

Equations (8) and (9), along with conditions (4), which determine the electron and hole chemical potentials, can be solved by successive approximations. The susceptibility of the excited sample can thus be calculated with the desired accuracy.

To determine the cubic susceptibility it is sufficient to consider the case of excitation levels at which the filling of only a pair of low-lying quantum-well levels is important. In this case the induced change in the susceptibility, $\Delta\chi = \chi - \chi_0$ (χ_0 is the linear susceptibility), can be written

$$\Delta\chi(\hbar\omega) = N_m \frac{|d_A|^2 2N}{(\hbar\omega - E_0) + i\hbar\Gamma_0}, \qquad (10)$$

where $E_0 = E_{A,0,1}$, and $\Gamma_0 = \Gamma_{A,0,1}$ [in (10), we have made use of the circumstance that when only the low-lying levels of the valence band and the conduction band are filled the corresponding occupation numbers n^e and n^h are equal to $N/2$]. Using the linear value of the susceptibility, χ_0, to determine N [see (9); this is the first step of a successive-approximation procedure], we find

$$\Delta\chi(\hbar\omega) = N_m \frac{4|d_A|^2 \tau_e |\operatorname{Im}\chi_0|}{\hbar[(\hbar\omega - E_0) + i\hbar\Gamma_0]} |E_\omega|^2, \qquad (11)$$

and thus

$$\chi^{(3)}(\hbar\omega)=\frac{\xi}{V_m}\frac{8|d_A|^4\tau_e\Gamma_0}{[(\hbar\omega-E_0)^2+\hbar^2\Gamma_0^2][(\hbar\omega-E_0)+i\hbar\Gamma_0]}. \quad (12)$$

In (12) we have considered only the first resonance of $\operatorname{Im}\chi_0$, since the denominator in (11) greatly reduces the contributions of the other resonances. In addition, the factor N_m is written as the ratio ξ/V_m in order to stress the strong dependence of $\chi^{(3)}$ on the volume of an individual microcrystal ($\chi^{(3)}\propto 1/V_m$). Consequently, in the case of small microcrystals (in which the exciton correlations are negligibly small), nonlinear susceptibilities increase rapidly with decreasing microcrystal radius (as $1/R^3$) if the concentration by volume of the semiconductor, ξ, remains constant.

For comparison with experiment, we use the amplitude value $|\operatorname{Im}\chi^{(3)}|$. From (12) we have

$$|\operatorname{Im}\chi^{(3)}|_{max}=\frac{\xi}{V_m}\frac{8|d_A|^4\tau_e}{\hbar^3\Gamma_0^2}. \quad (13)$$

For sample 1 we have $\tau_e=1.7$ ns, $R=6$ nm, $\xi=0.1\%$, $\hbar\Gamma_0=1.2\cdot10^{-13}$ erg ($\hbar\Gamma_0=3^{1/2}\Delta E/2$, where ΔE is the distance between the extrema in the $\operatorname{Re}\chi^{(3)}$ spectrum), and $d_A=2.4\cdot10^{-17}$ esu (for the oscillator strength of the exciton transition averaged over the polarization,[18] $\langle f_A\rangle=1.5\cdot10^{-3}$). We thus find $|\operatorname{Im}\chi^{(3)}|=3\cdot10^{-7}$ esu. This result is slightly higher than the experimental value, which is about $6\cdot10^{-8}$ esu. Note, however, that inhomogeneous-broadening effects, which were ignored in the derivation of (12), will reduce the calculated values of the nonlinear susceptibilities. It follows in particular that we should apparently use not the total concentration by volume of the microcrystals in (12) but only the concentration of "working" microcrystals, which is smaller by a factor of about Γ_0/Γ_i (Γ_i is the width of the inhomogeneous-broadening band). Using (13), we find the following expression for the ratio of the cubic susceptibilities of samples 1 and 2:

$$\frac{|\operatorname{Im}\chi_1^{(3)}|_{max}}{|\operatorname{Im}\chi_2^{(3)}|_{max}}=\frac{\xi_1\tau_1\Gamma_{02}{}^2R_2{}^3}{\xi_2\tau_2\Gamma_{01}{}^2R_1{}^3}.$$

It follows from this result that, despite the improvement in the values of $\chi^{(3)}$ due to the smaller radius of the microcrystals, the sharp reduction of the carrier lifetime and the increase in the broadening Γ_0 in the case of sample 2 lead to a resultant decrease in the cubic susceptibility, by a factor of nearly 60 (ξ_1/ξ_2 is about 2). This conclusion agrees with the experimental data (where we find the ratio of the measured values to be approximately 70).

In summary, we have used methods of nonlinear picosecond spectroscopy to successfully detect transitions between several pairs of quantum-well levels in semiconductor microcrystals (quantum dots). The results of measurements of the nonlinear transmission spectra have been used to determine the spectra of the real and imaginary parts of the cubic susceptibility. We have detected a decrease in the size of the nonlinearity with decreasing size of the microcrystals, due primarily to a sharp decrease in the carrier lifetime.

[1)] D. K. Okorokov and the present authors have recently detected lasing in sample 1, from which an optical cavity had been fabricated.

[1] Al. L. Éfros and A. L. Éfros, Fiz. Tekh. Poluprovodn. **16**, 1209 (1982) [Sov. Phys. Semicond. **16**, 772 (1982)].
[2] D. W. Hall and N. F. Borrelly, J. Opt. Soc. Am. **5**, 1650 (1988).
[3] D. Richard, P. Roussignol, C. Flytzanis, and N. Neutron, Physica A **157**, 437 (1989).
[4] Yu. V. Vandyshev, V. S. Dneprovskiĭ, A. I. Ekimov *et al.*, Pis'ma Zh. Eksp. Teor. Fiz. **46**, 393 (1987) [JETP Lett. **46**, 495 (1987)].
[5] D. S. Chemla and D. A. B. Miller, J. Opt. Soc. Am. B **2**, 1155 (1985).
[6] S. Schmitt-Rink, D. A. Miller, and D. S. Chemla, Phys. Rev. B **35**, 8113 (1987).
[7] E. Hanamura, Phys. Rev. B **37**, 1273 (1988).
[8] V. S. Williams, G. R. Olbright, B. D. Fluegel *et al.*, J. Mod. Opt. **35**, 1979 (1988).
[9] V. S. Dneprovskii, Al. L. Efros, A. I. Ekimov *et al.*, Solid State Commun. **74**, 555 (1990).
[10] K. Shum, G. C. Tang, R. Mahesh *et al.*, Appl. Phys. Lett. **51**, 1839 (1987).
[11] Yu. V. Vandyshev, V. S. Dneprovskiĭ, and V. I. Klimov, Pis'ma Zh. Eksp. Teor. Fiz. **53**, 301 (1991) [JETP Lett. **53**, 314 (1991)].
[12] I. M. Lifshitz and V. V. Slezov, Zh. Eksp. Teor. Fiz. **35**, 479 (1958) [Sov. Phys. JETP **8**, 331 (1959)].
[13] S. S. Yao, C. Karaguleff, A. Gabel *et al.*, Appl. Phys. Lett. **46**, 801 (1985).
[14] K. Nattermann, B. Danielzik, and D. von der Linde, Appl. Phys. A **44**, 111 (1987).
[15] P. Roussignol, D. Richard, and C. Flytzanis, Appl. Phys. A **44**, 285 (1987).
[16] I. R. Shen, *Principles of Nonlinear Optics*, Nauka, Moscow, 1989.
[17] L. G. Zimin, S. V. Gaponenko, I. E. Malinovskii *et al.*, Phys. Status Solidi (b) **159**, 449 (1990).
[18] J. Voight, F. Spiegelberg, and M. Senoner, Phys. Status Solidi (b) **91**, 189 (1979).

Translated by D. Parsons